

Solitons in two-dimensional lattices possessing defects, dislocations, and quasicrystal structures

Mark J. Ablowitz,¹ Boaz Ilan,² Ethan Schonbrun,³ and Rafael Piestun³

¹*Department of Applied Mathematics, University of Colorado, Boulder, Colorado 80309-0526, USA*

²*School of Natural Sciences, University of California, Merced, P.O. Box 2039, Merced, California 95344, USA*

³*Department of Electrical and Computer Engineering, University of Colorado, Boulder, Colorado 80309-0425, USA*

(Received 12 April 2006; published 7 September 2006; publisher error corrected 8 September 2006)

Localized nonlinear modes, or solitons, are obtained for the two-dimensional nonlinear Schrödinger equation with various external potentials that possess large variations from periodicity, i.e., vacancy defects, edge dislocations, and quasicrystal structure. The solitons are obtained by employing a spectral fixed-point computational scheme. Investigation of soliton evolution by direct numerical simulations shows that irregular-lattice solitons can be stable, unstable, or undergo collapse.

DOI: [10.1103/PhysRevE.74.035601](https://doi.org/10.1103/PhysRevE.74.035601)

PACS number(s): 05.45.Yv, 42.65.Tg, 63.20.Pw, 61.44.Br

Solitons are localized nonlinear waves that occur in many branches of physics and their properties have provided a deep and fundamental understanding of complex nonlinear systems. In recent years there has been considerable interest in the study of solitons in systems with periodic potentials or lattices, in particular those that can be generated in nonlinear optical materials [1–5]. In periodic lattices, solitons can form when their propagation constant, or eigenvalue, lies within certain regions, often called gaps, a concept that is borrowed from Floquet-Bloch theory for linear propagation. However, the external potential of complex systems can be much more general and physically richer than a periodic lattice. For example, atomic crystals can possess various irregularities, such as defects, and edge dislocations, as well as quasicrystal structures, which have long-range orientational order but no translational symmetry [6,7]. In general, when the lattice's periodicity is slightly perturbed, the band-gap structure and soliton properties become slightly perturbed as well, but otherwise solitons are expected to exist in much the same way as in the perfectly periodic case [8,9]. However, the existence and properties of multidimensional solitons when the external potential possesses large variations from periodicity has remained largely unexplored.

In this Rapid Communication, we find two-dimensional (2D) solitons in lattices possessing vacancy defects, edge-dislocations, and quasicrystal structures. This is achieved using a fixed-point spectral method for computing the ground states of the underlying nonlinear Schrödinger (NLS) equation. A comparative study of the power-eigenvalue dependence leads to important observations regarding soliton power, gap edge, and stability properties. Evolution is investigated by direct numerical simulations, showing that slightly perturbed solitary waves in irregular lattices can either undergo small or large amplitude oscillations or collapse. We note that the physical properties of optically generated quasicrystal potentials have generated significant interest and that vortex waves have recently been employed in the generation of localized defects within optical lattices [10,11]. Our results also have application to photonic band-gap systems, wherein novel experimental techniques have recently been used to fabricate irregular lattice structures [11–14].

We study the nonlinear system governed by the focusing (2+1)D NLS equation (in nondimensional units) with an external potential,

$$iu_z + \Delta u + |u|^2 u - V(x, y)u = 0. \quad (1)$$

In optics, $u(x, y, z)$ corresponds to a complex-valued slowly varying amplitude of the electric field in the (x, y) plane that is propagating along the z direction; $\Delta u \equiv u_{xx} + u_{yy}$ corresponds to diffraction, the cubic term in u originates from the nonlinear (Kerr) change in the refractive index, and the potential $V(x, y)$ corresponds to a modulation of the linear refractive index of the medium. Equation (1) also governs the dynamics of certain Bose-Einstein condensates (BEC), where $u(x, y, z)$ represents the wave function of the mean-field atomic condensate that is trapped in a potential [15].

We look for localized solutions of Eq. (1) in the form $u(x, y, z) = f(x, y)e^{-i\mu z}$, where μ is the propagation constant (or eigenvalue) and $f(x, y)$ is a real-valued localized function that, following Eq. (1), satisfies the nonlinear eigenequation

$$\Delta f + [\mu + |f|^2 - V(x, y)]f = 0. \quad (2)$$

In this study we consider potentials that can be written as the intensity of a sum of N phase-modulated plane waves, i.e.,

$$V(x, y) = \frac{V_0}{N^2} \left| \sum_{n=0}^{N-1} e^{i\vec{k}_n \cdot \vec{r} + i\theta_n(x, y)} \right|^2, \quad (3)$$

where $V_0 > 0$ is constant, $\vec{r} = (x, y)$, \vec{k}_n is a wave vector, $\theta_n(x, y)$ is a phase function through which irregularities are introduced, and the normalization by N^2 gives that V_0 is the potential's peak depth, i.e., $V_0 = \max_{x, y} V(x, y)$. Such 2D potentials can be physically realized in optics by interference of plane waves and phase functions [11]. In some situations, they are invariant in the third dimension (3D) [16]. For example, these phase functions can be composed from different configurations of vortices [17], which, in turn, can be created using computer-generated holograms [11].

In order to solve Eq. (2), we use a fixed point spectral computational method [18], as explained below. Applying the Fourier transform to Eq. (2) and adding and subtracting a term $r\hat{u}$, where $r > 0$ is constant, leads to

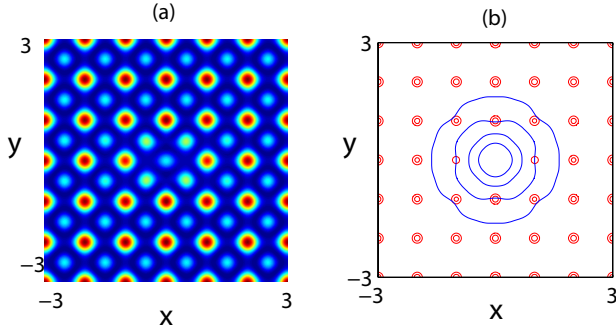


FIG. 1. (Color online) (a) Contour image of a lattice with a vacancy defect, i.e., Eq. (4) with $K=k_x=k_y=2\pi$ and $V_0=12.5$. Spots correspond to local maxima. (b) Contour plot of the soliton with $\mu=0.5$ superimposed on the lattice. For visibility, only a small portion of the $[-10, 10]^2$ computational domain is presented.

$$\hat{f}(\nu) = \hat{R}[\hat{f}] \equiv \frac{(r + \mu)\hat{f} + \mathcal{F}\{[|f|^2 - V(x, y)]f\}}{r + |\nu|^2},$$

where $\nu=(\nu_x, \nu_y)$ are the Fourier variables, \mathcal{F} stands for the Fourier transform, and the role of the constant r is to avoid a singularity in the denominator (we use $r=5$). A new field variable is introduced as $f(x, y)=\lambda w(x, y)$, where $\lambda \neq 0$ is a constant to be determined. The iteration method takes the form $\hat{w}_{m+1}=\lambda_m^{-1}\hat{R}[\lambda_m\hat{w}_m]$, $m=0, 1, 2, \dots$, where λ_m satisfies the associated algebraic condition

$$\int \int_{-\infty}^{+\infty} |\hat{w}_m(\nu)|^2 d\nu = \lambda_m^{-1} \int \int_{-\infty}^{+\infty} \hat{R}[\lambda_m\hat{w}_m]\hat{w}_m^*(\nu) d\nu.$$

It has been found that this method prevents the numerical scheme from diverging. Thus, the soliton is obtained from a convergent iterative scheme (see also [19] for an alternative procedure in case there is a well-defined homogeneity). The initial “starting point,” $w_0(x, y)$, is typically chosen to be a Gaussian. The iterations are stopped when the relative convergence factor, $\delta=|(\lambda_{m+1}/\lambda_m)-1|$, reaches 10^{-10} . We note that convergence is reached quickly, but slows down as the mode becomes more extended, i.e., as μ approaches the (nonlinear) gap edge. We also note that the convergence of a similar method has been proven under suitable assumptions on the potential [20].

The first case of the potential (3) we study is an irregular 2D square lattice with a vacancy defect [see Fig. 1(a)], i.e.,

$$V(x, y) = \frac{V_0}{25} |2 \cos(k_x x) + 2 \cos(k_y y) + e^{i\theta(x, y)}|^2, \quad (4)$$

where the phase function $\theta(x, y)$ is given by

$$\theta(x, y) = \tan^{-1}\left(\frac{y-y_0}{x}\right) - \tan^{-1}\left(\frac{y+y_0}{x}\right).$$

Physically, $\theta(x, y)$ corresponds to two first-order phase dislocations displaced in the y direction by a distance of $2y_0$. A vacancy defect can thus be obtained using $y_0=\pi/K$, where $K=k_x=k_y$. Note that the “vacancy” in the origin is created from a continuous function and that far from the origin the

potential (4) is locally a square lattice with period $2\pi/K$. Using the computational method outlined above, localized modes (solitons) of Eqs. (2) and (4) are found, centered around the vacancy as shown in Fig. 1(b). In certain respects, they resemble solitons centered around a minimum of a periodic square lattice. In further investigations, it is found that as the soliton’s center is moved farther from the vacancy, its profile and band-gap structure converge to those of the corresponding periodic lattice [i.e., Eq. (4) with $\theta(x, y)\equiv 0$].

In a similar manner, a lattice with an edge dislocation, analogous to those that can be found in atomic crystals [7,11], can be obtained from Eq. (3) using

$$V(x, y) = \frac{V_0}{25} \{2 \cos[k_x x + \theta(x, y)] + 2 \cos(k_y y) + 1\}^2, \quad (5)$$

with the phase-dislocation function $\theta(x, y)=\frac{3\pi}{2}-\tan^{-1}\left(\frac{y}{x}\right)$. Figure 2(a) shows that this dislocation is unlike a point defect, insofar as the density of lattice sites changes vertically across the lattice. Despite this strong irregularity, solitons are found to exist in the vicinity of the phase dislocation. Figure 2(b) shows that the soliton has an asymmetric shape. The soliton’s center is situated above the phase dislocation, in between neighboring local maxima of the lattice. In this respect, it is like a soliton on a lattice minimum. It should be noted that the starting point of the computational method is around the origin and, during the iterations, the solution moves upward along the y axis, until convergence is reached.

Next we investigate solitons on quasicrystal lattices. Such lattices appear naturally in certain molecules [6,7], have been investigated in optics [21–23] and studied in BEC [24]. Importantly, Freedman *et al.* recently predicted and observed solitons in Penrose quasicrystals, which were generated using the method of optical induction [25]. In this study, the optical potential is formed by the far-field diffraction pattern of a mask with point apertures that are located on the N vertices of a regular polygon. The corresponding potential is given by

$$V(x, y) = \frac{V_0}{N^2} \left| \sum_{n=0}^{N-1} e^{i(k_x x + k_y y)} \right|^2, \quad (6)$$

where $(k_x, k_y)=(K \cos(2\pi n/N), K \sin(2\pi n/N))$. The potential (6) with $N=2, 3, 4, 6$ yields periodic lattices, which cor-

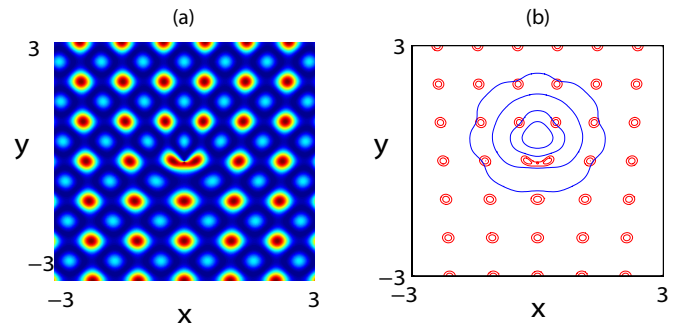


FIG. 2. (Color online) Same as Fig. 1 for a lattice with an edge dislocation [Eq. (5)], using the same lattice parameters and $\mu=0.5$ as in Fig. 1. The soliton’s peak is located at $(0, 0.68)$.

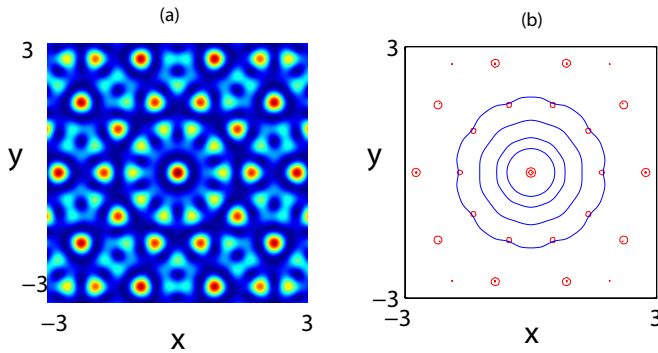


FIG. 3. (Color online) Same as Fig. 1 for a Penrose lattice [Eq. (6) with $N=5$] and corresponding soliton centered around the center (maximum), using the same lattice parameters and $\mu=0.5$ as in Fig. 1.

respond to the standard 2D crystal structures. All other values of N correspond to quasicrystals, which have a local symmetry around the origin and long-range order, but, unlike periodic crystals, are not invariant under spatial translation [26]. Below we focus on the case $N=5$ [see Fig. 3(a)], whose lattice is often referred to as a Penrose quasicrystal.

We find solitons on the Penrose lattice [see Fig. 3(b)], centered around the origin, which is the global maximum of the lattice potential. Similar to solitons centered at the maximum of a periodic square lattice, these Penrose solitons have a dimple (see Fig. 4). Further investigations reveal that Penrose solitons centered around local minima do not have a dimple, similar to their periodic-lattice counterparts.

It is noteworthy that in the limit of waves impinging from all directions (i.e., $N \rightarrow \infty$), the quasicrystal lattice (6) approaches the Bessel lattice, i.e., $\lim_{N \rightarrow \infty} V(x,y;N) = V_0 J_0^2(Kr)$, in which solitons have recently been studied (cf. [27]). In fact, as N increases, at any given radius the angular distance between the lattice maxima (and minima) decreases and the limiting Bessel lattice has continuous rings of maxima.

We note that some of the previous studies of Penrose lattices considered a different definition of the lattice, whereby cylinders of Kerr material were located at vertices

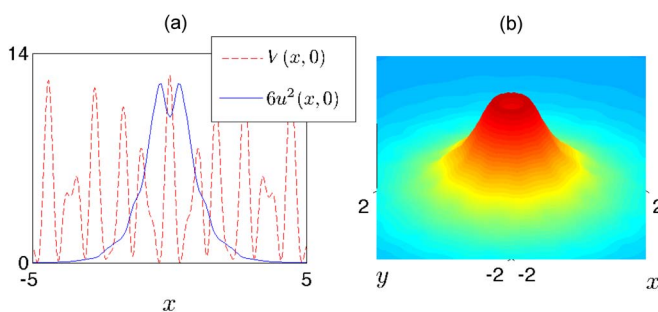


FIG. 4. (Color online) Similar to solitons on the maxima of periodic lattices, Penrose solitons can have a dimple, which becomes more pronounced for large values of μ , i.e., near the gap edge. (a) Cross section along the y axis of a Penrose soliton [$6u^2(x,0)$, solid] with $\mu=2$, superimposed on the underlying lattice (dashes). (b) 3D view of a soliton's intensity showing the dimple.

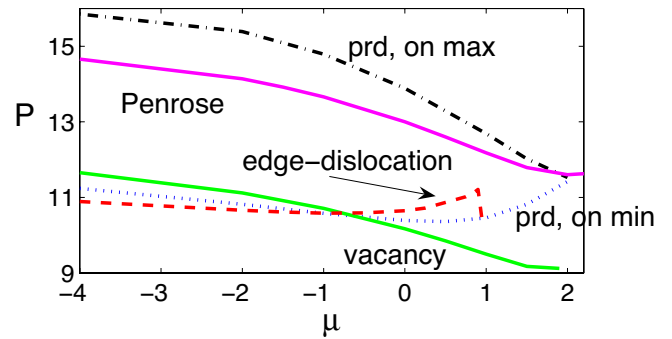


FIG. 5. (Color online) Soliton power as a function of eigenvalue within the semi-infinite band gap, for the same lattices as in the previous figures, as well as solitons on the maximum and minimum of a periodic (prd) square lattice. All lattices share a common peak depth, $V_0=12.5$, and background periodicity, $K=2\pi$.

of a (virtual) Penrose tile surrounded by air [21–23,28,29]. In contrast, the medium considered here is homogeneous, with a constant Kerr coefficient and continuous modulation of the linear refractive index (6).

To compare the different lattice solitons, in Fig. 5 we plot the soliton power, $P = \int |u|^2 dx dy$, as a function of eigenvalue μ , for all the lattices studied above, as well as for the corresponding periodic square lattice [i.e., Eq. (4) with $\theta(x,y) \equiv 0$] centered around either local minima and maxima. We remark that all the above lattices share a common peak depth, $V_0=12.5$, as well as periodicity far from the irregularity, $K=2\pi$, where for the Penrose lattice K can be thought of as a “local” wave number [see Eq. (6)].

We define the first nonlinear gap edge μ_{\max} as the minimal eigenvalue beyond which the numerical method does not converge to a localized state. The comparison shows that all the lattices above have a semi-infinite gap, i.e., the numerical method converges to a localized state when $\mu < \mu_{\max}$, for some lattice-dependent μ_{\max} . When the eigenvalue exceeds μ_{\max} , the numerical method typically converges to an extended state (but see below for exceptions). In addition, the comparison reveals that (see Fig. 5) (i) the power of vacancy-defect, edge-dislocation, and Penrose-quasicrystal lattice solitons is lower than their periodic counterparts for a considerable range of eigenvalues. In particular, of all the lattices studied here, the lowest power is obtained for vacancy and edge-dislocation solitons. (ii) A vacancy defect has little effect on the gap size ($\mu_{\max} \approx 2$), but it significantly reduces the power threshold, i.e., the minimal soliton power throughout the gap. However, it is noteworthy that the power threshold is positive for all these potentials, i.e., the irregularities do not allow the formation of linear (zero-power) modes within the gap. (iii) An edge dislocation reduces the gap size (note: $\mu_{\max} \approx 0.95$), whereas (iv) a Penrose soliton has a slightly larger gap size ($\mu_{\max} \approx 2.2$) compared to a soliton on a periodic square lattice. However, solitons on the maxima of periodic-square and Penrose lattices have a similar power behavior, which is a somewhat unexpected result, since these lattices have a very different structure.

A striking observation in Fig. 5 is that the gap edge with an edge dislocation occurs at $0.9 < \mu_{\max} < 0.95$, which is considerably smaller than for the other lattices. In fact, during the computation, an interesting phenomenon occurs as μ is increased. When $\mu=0.9$, a reliable convergence ($\delta=10^{-10}$) is reached and, in this case, the solution is between the local maxima shown in Fig. 2(b). When $\mu=0.95$, the solution initially converges at the same location (with $\delta=10^{-5}$). However, this convergence is misleading, since with further iterations the solution moves upward along the y axis, “sliding” up in between two local maxima and eventually converging (with $\delta=10^{-10}$) in between the four local maxima that are one lattice cell above the edge dislocation. The resulting soliton is therefore similar to one on a periodic square lattice, insofar as the nearest four lattice maxima are approximately symmetric and equispaced. In fact, further investigations reveal that for $0.95 < \mu < 2$ the soliton remains one lattice cell above the dislocation and its power-eigenvalue dependence is very similar to that on a periodic lattice. Thus, the edge dislocation clearly shrinks the size of the nonlinear gap.

The question of soliton evolution under perturbations is

important for applications. To study this, we perform direct computations of Eq. (1) using the various potentials, where the initial conditions are the solitons with 1% random noise in amplitude and phase. Generically, it is found that (i) solitons centered around lattice minima (e.g., of periodic, vacancy, edge-dislocation, and quasicrystal lattices) undergo small-amplitude oscillations when $dP/d\mu < 0$ and large-amplitude oscillations when $dP/d\mu > 0$; (ii) solitons centered around lattice maxima (e.g., of periodic and quasicrystal lattices) can undergo collapse after a finite propagation distance.

In conclusion, the existence of stable 2D solitons is demonstrated in self-focusing media with irregular lattice potentials, possessing vacancy defects, dislocations, and quasicrystal structures. Figure 5 shows that these Penrose solitons are similar to solitons on the periodic-lattice maxima, whereas there are significant differences between vacancy and edge-dislocations solitons as compared to their periodic-lattice counterparts.

This work was partially supported by US Air Force under Grant No. F-49620-03-1-0250.

-
- [1] D. N. Christodoulides, F. Lederer, and Y. Silberberg, *Nature (London)* **424**, 817 (2003).
- [2] A. A. Sukhorukov, Y. S. Kivshar, H. S. Eisenberg, and Y. Silberberg, *IEEE J. Quantum Electron.* **39**, 31 (2003).
- [3] N. K. Efremidis, J. Hudock, D. N. Christodoulides, J. W. Fleischer, O. Cohen, and M. Segev, *Phys. Rev. Lett.* **91**, 213906 (2003).
- [4] J. W. Fleischer, M. Segev, N. K. Efremidis, and D. N. Christodoulides, *Nature (London)* **422**, 147 (2003).
- [5] D. Neshev, Y. S. Kivshar, H. Martin, and Z. Chen, *Opt. Lett.* **29**, 486 (2004).
- [6] D. Shechtman, I. Blech, D. Gratias, and J. W. Cahn, *Phys. Rev. Lett.* **53**, 1951 (1984).
- [7] M. P. Marder, *Condensed Matter Physics* (Wiley-Interscience, New-York, 2001).
- [8] F. Fedele, J. Yang, and Z. Chen, *Stud. Appl. Math.* **115**, 279 (2005).
- [9] H. Buljan, G. Bartal, O. Cohen, T. Schwartz, O. Manela, M. Segev, T. Carmon, J. W. Fleischer, and D. N. Christodoulides, *Stud. Appl. Math.* **115**, 173 (2005).
- [10] L. Guidoni, C. Triché, P. Verkerk, and G. Grynberg, *Phys. Rev. Lett.* **79**, 3363 (1997).
- [11] E. Schonbrun and R. Piestun, *Opt. Eng. (Bellingham)* **45**, 028001 (2006).
- [12] T. Pertsch, U. Peschel, F. Lederer, J. Burghoff, M. Will, S. Nolte, and A. Tünnermann, *Opt. Lett.* **29**, 468 (2004).
- [13] M. Qi, E. Lidorikis, P. T. Rakich, S. G. Johnson, J. D. Joannopoulos, E. P. Ippen, and H. I. Smith, *Nature (London)* **429**, 538 (2004).
- [14] W. Cai and R. Piestun, *Appl. Phys. Lett.* **88**, 111112 (2006).
- [15] C. J. Pethick and H. Smith, *Bose-Einstein Condensation in Dilute Gases* (Cambridge University Press, Cambridge, England, 2001).
- [16] R. Piestun and J. Shamir, *J. Opt. Soc. Am. A* **15**, 3039 (1998).
- [17] J. F. Nye and M. V. Berry, *Proc. R. Soc. London, Ser. A* **336**, 165 (1974).
- [18] M. J. Ablowitz and Z. H. Musslimani, *Opt. Lett.* **30**, 2140 (2005).
- [19] Z. H. Musslimani and J. Yang, *J. Opt. Soc. Am. B* **21**, 973 (2004).
- [20] D. E. Pelinovsky and Y. A. Stepanyants, *SIAM J. Appl. Math.* **42**, 1110 (2004).
- [21] R. T. Bratfalean, A. C. Peacock, N. G. R. Broderick, K. Gallo, and R. Lewen, *Opt. Lett.* **30**, 424 (2004).
- [22] R. Lifshitz, A. Arie, and A. Bahabad, *Phys. Rev. Lett.* **95**, 133901 (2005).
- [23] W. Man, M. Megens, P. J. Steinhart, and P. M. Chaikin, *Nature (London)* **436**, 993 (2005).
- [24] L. Sanchez-Palencia and L. Santos, *Phys. Rev. A* **72**, 053607 (2005).
- [25] B. Freedman, G. Bartal, M. Segev, R. Lifshitz, D. N. Christodoulides, and J. W. Fleischer, *Nature (London)* **440**, 1166 (2006).
- [26] M. Senechal, *Quasicrystals and Geometry* (Cambridge University Press, Cambridge, England, 1995).
- [27] Y. V. Kartashov, V. A. Vysloukh, and L. Torner, *Phys. Rev. Lett.* **93**, 093904 (2004).
- [28] P. Xie, Z.-Q. Zhang, and X. Zhang, *Phys. Rev. E* **67**, 026607 (2003).
- [29] A. Della Villa, S. Enoch, G. Tayeb, V. Pierro, V. Galdi, and F. Capolino, *Phys. Rev. Lett.* **94**, 183903 (2005).